Available online at www.sciencedirect.com

ScienceDirect

Procedia CIRP 37 (2015) 77 – 82

www.elsevier.com/locate/procedia

CIRPe 2015 - Understanding the life cycle implications of manufacturing

Particle speed analysis in CoBlast

C. Stenson[a], M. C. Meyer[a], B. Twomey[b] and R. Lupoi[a]*

[a]*Trinity College Dublin, the University of Dublin, Department of Mechanical and Manufacturing Engineering, Parsons Building, Dublin 2, Ireland*
[b]*ENBIO, Nova UCD, Belfield Innovation Park, University College Dublin, Belfield, Dublin 4, Ireland*

* Corresponding author: Tel.: +353-1-8961729; E-Mail: lupoir@tcd.ie

Abstract

The deposition of well-adhered thin type of coatings is of great importance in manufacturing and is used in numerous applications. Of particular interest in the biomedical sector is the deposition of hydroxyapatite onto titanium. CoBlast is a novel coating technology used mainly in the deposition of ceramics onto this metal. This is achieved by simultaneously blasting a ceramic particulate (the abrasive) and coating particles (the dopant) at a substrate with the resulting impregnation of the coating particles onto the substrate surface. The goal of this research was to investigate the velocities achieved by the abrasive particles under typical process pressures using a CoBlast nozzle. The velocity measurements were carried out using Particle Image Velocimetry by which method 200µm aluminium oxide powder was investigated at pressures of 3, 4 and 5 bar at variable mass flow rates. Computational Fluid Dynamics using ANSYS-Fluent was used to predict the particle dynamics and results were compared to those obtained by the experiments. It was possible to generate valuable experimental data that provide an initial mean for process characterization and for the design of new and more efficient CoBlast nozzles.

Peer-review under responsibility of the organizing committee of CIRPe 2015 - Understanding the life cycle implications of manufacturing

Keywords: CoBlast; Particle Image Velocimetry (PIV); Computational Fluid Dynamics; Particle Speed; Alumina.

1. Introduction

The range of applications for thin coating deposition techniques is large. Coatings deposited using chemical vapour deposition (CVD) or physical vapour deposition (PVD) offer extreme precision in terms of coating composition, microstructure and thickness[1]–[3]. This level of control is necessary in applications such as deposition of silicon in the semiconductor industry and applying thermal barrier coatings onto turbine blades[4]. In these methods, very precise regulation of process parameters is necessary. For example, maintaining vacuums or gas flow rates. As such, the equipment and expertise requirements and therefore the costs are considerable[5]. CoBlast is a novel ad ambient temperature thin coating deposition process, proprietary of EnBio. Its simplicity and economy comes from its modest equipment needs. No special temperature, pressure, or inert environments are involved[6]. However, this comes with disadvantages in terms of the controllability compared to CVD and PVD. The CoBlast process, schematically described in Figure 1, involves the simultaneous blasting of a coating material (or dopant) and abrasive particles (typically alumina) at a substrate using pressurised air.

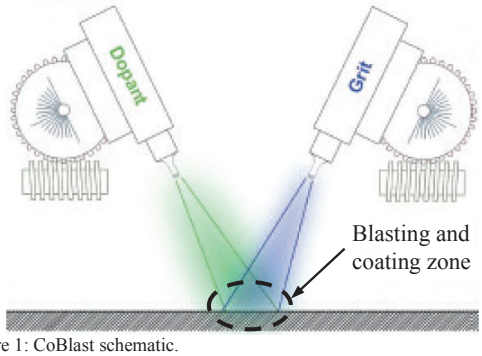

Figure 1: CoBlast schematic.

Peer-review under responsibility of the organizing committee of CIRPe 2015 - Understanding the life cycle implications of manufacturing
doi:10.1016/j.procir.2015.08.004

This can be carried out either with two separate streams, one for coating particles and one for abrasive particles, or combining both in a single jet. When a single stream is used the particles are mixed in a hopper and are then fed to a de Laval nozzle. The adhesion which occurs is a result of both tribochemical bonding and mechanical interlocking[7], [8]. The first part of the process involves the abrasive particles impinging on the substrate where they disrupt and erode the oxide layer on the surface. This exposes some of the pure metal underneath and significantly roughens it[8], [9]. The abrasive particles also shatter the coating particles, the kinetic energy of which cause a tribochemical bond to form with the exposed highly reactive metal. This results in the formation of a surface layer which is folded into the substrate metal[10], [11]. The folding happens due to the high surface area and irregular morphology of the roughened and exposed, pure metal[8], [9]. This intricate mechano-chemical surface structure results in the interlocking between the coating and substrate which strengthens the adhesion[12]. The end result is a substrate which has been thoroughly covered in a strongly adhered but thin (2-5 μm) layer of the desired coating material.

One of the most common applications of CoBlast is the deposition of hydroxyapatite onto titanium for medical implantation. The roughness of the resulting surface is extremely important for successful integration[13], [14]. The role of abrasive particle kinetic energy in erosion and resulting surface structure is well documented [7], [9]. Given the importance of particle kinetic energy in the tribochemical bond formation it is clear that particle velocity is of great influence to the CoBlast process. It is in fact fundamental to understand the particle velocity range needed for bonding to occur, currently unknown. Separate research is being carried out focusing on the substrate and examining the relationship between abrasive and coating particle kinetic energy and the resulting surface roughness and coating thickness.

This paper is aimed at determining the velocities which are currently being achieved using CoBlast nozzles at common working pressures reported in [9], [16]. With a better understanding of the particle kinetics using numerical and experimental methods, it will be possible to understand the critical speed for deposition, currently unknown. This will lead to the design of tailor made nozzles to achieve the same threshold velocities, however using different geometries, for example longer or shorter nozzle, so as to adapt to each application case with the aim of improving process efficiency.

Velocity was investigated in the region stretching from the nozzle exit to the distance of the substrate, 50mm away. The velocity measurements were taken using Particle Image Velocimetry (PIV) and results were averaged over the region of interest. The measurements were compared with simulations created using the Computational Fluid Dynamics (CFD) package ANSYS Fluent v14.5. The intention of the computer modelling was to investigate the accuracy of the software at simulating the physics of the process.

2. Particle Image Velocimetry

PIV was chosen as the method of taking velocity measurements of the aluminum oxide particles. This work is focuses in the first place in the abrasive only speed, hence the feedstock is not mixed with the active or coating phase. In PIV operations, there are a number of considerations which must be observed in order to obtain accurate measurements and to minimise the potential errors. The number of light scattering particles which can be seen in each recorded image, called ‘image density’ is key[17]. Image density can be low, medium or high. Low image density usually involves one particle per 32 x 32 pixel interrogation window[18]. The light scattering behavior of the particles is another important consideration as laid out by Raffel et al[17]. Depending on the reflected and incident light angles from a particle, variations of several orders of magnitude in recorded light intensity are experienced. Increase of scattered light intensity is also caused by increasing cross-section of the particles. As such, it is desirable to have particles of uniform size and shape so that light scattering behavior will be predictable. Then, achieving the desired image density of particles with appropriate image size and intensity becomes more practical. A preferable particle-image size is two pixels. This allows adequate resolution of the displacement to sub-pixel accuracy without causing excessive noise. It is known that noise increases with particle-image size, mainly due to the error in associating the correct pixel with the centre of the particle[17], [21]. The two other features of PIV which directly affect image quality are the camera lens and the light sheet. It is important that an appropriate camera lens is chosen and focused so that only particles which are properly illuminated and clearly defined within the light-sheet thickness will be imaged. The time-step between illuminations must be appropriate. Increasing it can reduce the percentage error in locating the particles centre. However, this is limited as it reduces the chances that a particle will be illuminated and recorded twice in succession. If the time-step is reduced, to ensure that particles are illuminated twice, size of the displacement is reduced. Often this value requires iteration for optimisation[17].

3. CFD for particle tracking

CFD was used to model the gas flow in the CoBlast nozzle, and to predict the particle dynamic behavior during the acceleration process.

The k-ε turbulence model is a two-equation turbulence model which uses the Boussinesq hypothesis to solve RANS. This means that it is assumed that turbulent viscosity is isotropic and Reynolds stresses can therefore be related to mean velocity gradients[22]. The k-ε model is relatively robust and provides accurate results in thin shear layer flows. It is also relatively computationally inexpensive[23]. However, there are some drawbacks to its use which mainly arise due to the incorrect assumption of isotropic turbulent viscosity. In particular, it is not very effective at predicting the spreading rate of axisymmetric jets[22]. To limit this, non-linear versions of the k-ε model have been developed. One of these is the ‘Realisable’ k-ε which has been validated for many different flows including free flows and jets.

The Discrete Phase Modelling (DPM) was used as means of obtaining particle speed data. It uses an Euler-Lagrange approach to calculate particle trajectories and velocities. The fluid flow is first solved and then the force over the particles

is integrated. The model consists of a discrete phase which in this case was the aluminium oxide particles, and a continuous phase which was the pressurised air. DPM gives the option of whether or not to account for the effect of the particles on the flow. One-way coupling integrates the force on the particles due to the flow at each point on the grid without the discrete phase having any effect on the continuous phase. Two-way coupling partially accounts for the effects of both. The force on the particles is integrated every set number of continuous phase iterations. The continuous phase is then iterated, taking into account the presence of the discrete phase. This is carried out until a converged, stable solution is reached. When one-way coupling is enabled this removes many of the random fluctuations which cause particle motion in directions other than the mean flow direction[23].

A critical assumption is that the volume fraction of the discrete phase is between <10% of the flow volume. As such, particle-particle interactions are unlikely to occur and are not included as part of the model[23]. This means the algorithm has no ability to predict the onset of choking. There are different ways to model the discrete phase in the DPM manifested by a selection of drag laws. The default option is the spherical drag law which assumes the particles are smooth spheres. The non-spherical drag law uses a dimensionless shape factor to account for the deviation of the particle shape from that of a smooth sphere. The shape factor is equal to the surface area of a sphere with the same volume as the particle divided by the actual surface area of the particle. A high Mach number drag law which is based on the spherical drag law has corrections which apply when the Mach number exceed 0.4 and the particle Reynolds number is larger than 20[23].

4. Measurements and Simulations set up

4.1. Equipment

The nozzle used in the experiments was a CoBlast nozzle supplied by EnBio. It is a converging-diverging De-Laval type of design made out of steel, with an inlet diameter of 9mm which decreased to 2.2mm at the throat (or restriction) over an 85mm length. The exit is slightly wider than the throat at 3mm diameter at the end of a 150mm long section.

A commercial powder feeder with a touch screen interface (Uniquecoat – wheel type) was used to supply the aluminium oxide. The gas and powder mixture from the feeder feeds directly in the nozzle inlet. The PIV equipment in Trinity College Dublin consisted of a CCD camera made by LaVision and a Solo II PIV water-cooled laser. The laser was connected to a timing unit which ensured the laser and camera triggered in the correct sequence. The software used to control the timing unit and to carry out the post-processing was the Data acquisition and Visualisation (DaVis) package, version 7.2, from LaVision. Relevant specifications of the camera and laser are given in table 1. The optics consisted of a mirror, a spherical focusing lens with a focal length of about 200mm, and a cylindrical sheet forming lens. These were held in place on adjustable pillars.

Table 1. PIV camera and laser specifications.

Camera		Laser	
Resolution	1280 x1024	Wavelength [nm]	532
Repetition [Hz]	8	Energy [mJ]	100
Pixel size [µm]	6.7x6.7	Pulse length [ns]	6
Minimum Δt [ns]	200	Beam diameter [mm]	3
Dynamic range	12 bit	Max. repetition rate [Hz]	15

A compressed air source was connected to the nozzle via the feeder. This could be controlled using a regulator and had a maximum pressure of 5.5 bar. An analogue gauge was placed at the nozzle inlet to give appropriate stagnation pressure readings. All of the equipment was put in place on a rig of aluminium profiles which was designed for such PIV applications. A polycarbonate containment unit was also used to prevent the escape of abrasive powder. This consisted of a long thin section where the measurements were taken and a larger section where most of the powder accumulated after testing. The detail of the PIV testing apparatus is shown in Figure 2. The laser beam is directed towards the nozzle by a series of mirrors and lenses, while a stream of particles injected from the feeder is exiting the nozzle. Two light flashes occur at a given time step; the particles reflection is captures by a high speed camera. The images are therefore analyzed and filtered by a software so as to obtain particle velocity recordings.

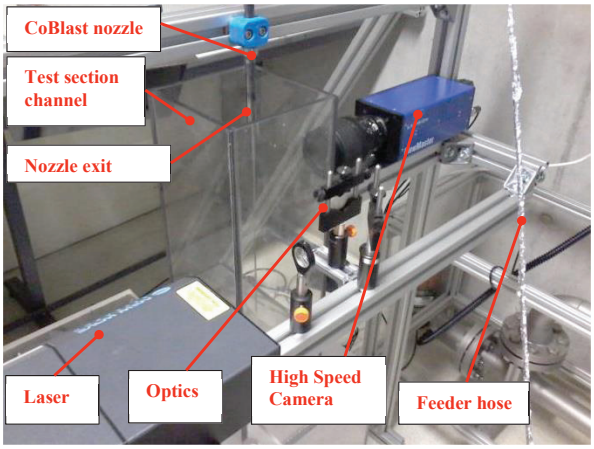

Figure 2: PIV apparatus for CoBlast particle speed measurements.

4.2. PIV measurements setup

PIV measurements were taken using aluminium oxide powder of 200µm nominal size at 3, 4 and 5 bar with a time-step of 5 µs. The particle mass flow rate estimates were obtained by collecting and weighting the sprayed material over the testing period. 240 image pairs were taken at a rate of 4Hz at each pressure over a range of mass flow rates. The procedure went as follows:

- Air flow was turned on and allowed to stabilize at the correct pressure. The powder feeder was set at constant wheel speed.
- After a settle time (approximately 5 seconds) the PIV recordings started.

- Measurements would carry on for an additional 60 seconds.
- The mass of powder collected in the test section was measured.

Once the measurements were taken they were post-processed using the DaVis software. This was carried out by first identifying all of the particle-image pairs by visual inspection. Parameters such as interrogation window shift and particle size range were input to try and locate these pairs. The success of the parameters was judged by the number of particle-image pairs which were detected by the software and could also be identified by visual inspection. When post-processing was carried out to satisfaction, the results were exported in the 'LaVison Davis 6 set' file format. These could be read into Matlab where a simple mean of the velocity vectors in each image was taken. A simple mean of these results was also taken to give the average velocity over the flow region at each pressure and mass flow rate.

4.3. CFD Simulations

The geometry constructed for the CFD simulations was created using the ANSYS software. The simulations were run in 2D for simplicity, and symmetry was used to reduce computational expense. The domain consisted of the nozzle interior as well as the region stretching 100mm from the nozzle exit and 30mm from its axis. A high quality mesh was constructed over this region. The mesh contained 45,240 nodes and 43,500 elements. Areas of high mesh density included the nozzle throat, nozzle exit and potential cone region.

The flow was solved as a steady-state problem using the density based solver. The continuous phase fluid was air with ideal gas density, constant specific heat and Sutherland viscosity. The "Realisable k-ε" turbulence model was used with standard wall functions. The wall functions meant the desired y^+ values were between 30 and 300. The non-spherical drag law was used. The particle size was assumed to be constant at 200µm. A shape factor for the non-spherical drag law was estimated from SEM images of the powder. The value used was 0.42393. The aluminium oxide properties were not present in the ANSYS library and were therefore taken from CES Edupak 2014. The density was taken as 3800 kg/m^3 and the specific heat was taken as 805kJ/kgK. It was also assumed that the particles started from rest and were released from each node of the inlet surface. Using one-way coupling simulations were run at 3, 4 and 5 bar inlet nozzle pressure.

5. Results and Discussion

5.1. PIV and CFD

The particle shown in Figure 3 was approximated as a triangular pyramid for calculating the DPM shape factor. It is very angular and quite irregular in shape. Further SEM images showed a wide range of particle shapes and sizes all of which were very irregular and inconsistent. It is clear that these particles were not conducive to predictable light scattering behavior. Prediction of both the scattering angle and cross-section was close to impossible.

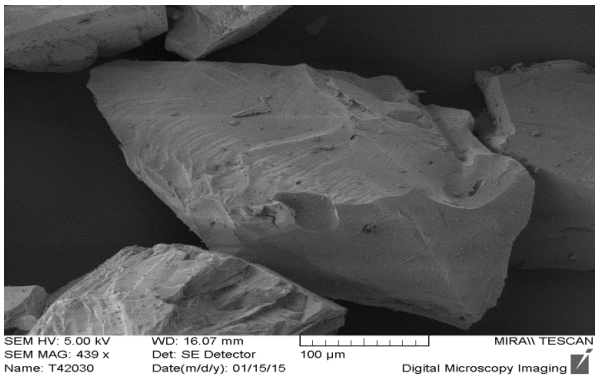

Figure 3: SEM image of alumina powder.

A comparison between the PIV measurements and CFD predictions is shown in Figure 4 and the results summarized in Table 2. The velocity achieved by the abrasive particles in CoBlast is in the region between 154.1 m/s and 188 m/s depending on mass flow rate and inlet pressure. The calculated error in the experimental measurements was +-4%. The mass flow rates which were measured in the testing were between 20.9 g/min and 160.1 g/min., as shown in Figure 3, with an error of approximately +-2%. These variations were obtained by changing the wheel speed of the feeder, hence allowing for more or less powder in the nozzle. The feeder is not equipped with a weight loss closed loop system; as a consequence when repeating an experiment with the same wheel settings there is no control on the actual powder feed rate. In a first instance, results compare well against the findings by Settles and Garg for velocity of 70µm aluminium particles in a de Laval nozzle[25], however those refer to a different process.

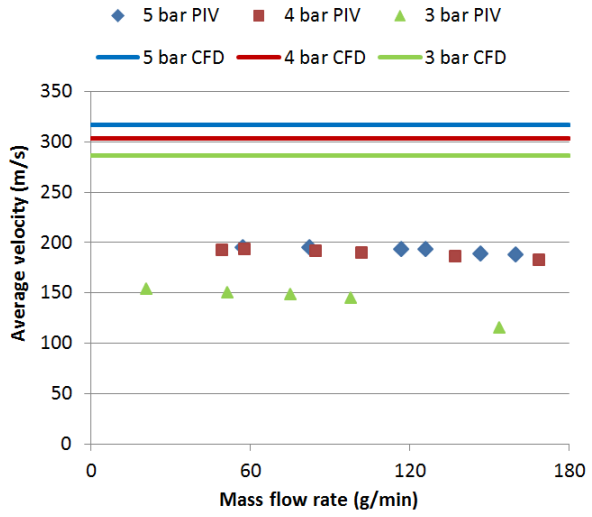

Figure 4: Particle stream average speed at nozzle exit vs. particle mass flow rate using PIV and CFD. Particle measurements were taken from the exit to 50mm downstream the nozzle.

Table 2. Velocity results (PIV) against particle mass flow rate measurements.

3 bar		4 bar		5 bar	
ṁ [g/min]	Velocity [m/s]	ṁ [g/min]	Velocity [m/s]	ṁ [g/min]	Velocity [m/s]
20.9	154.1	49.4	192.1	57.1	195.5
51.4	150.4	57.9	193.7	82.3	194.9
75.3	148.9	84.8	191.8	117.0	193.1
98.1	145.4	102.1	189.9	126.1	193.0
154	115.2	137.4	186.1	146.9	189.1
		168.9	182.5	160.1	188

The trend of decreasing average particle velocity with increasing mass flow rate when using PIV emerged, especially in the 3 bar case. The explanation for such behavior is related to the nozzle gas dynamics. As the particle loading increases, the particulate will occupy a higher volume fraction. This effect is magnified at the nozzle restriction or throat, where a relative high concentration of the solid phase can generate chocking conditions, resulting in a much reduced gas exit speed i.e. particle achievable velocity. A similar effect is observed for 4 and 5 bar, however in this case the velocity distribution variation with particulate mass flow rate appear less severe. A more comprehensive analysis is required to understand the reasons of why at higher level of inlet pressure different experimental observations were made. On the other hand, theoretical (CFD) results are not in well with the experimental measurements. The velocity levels are over-predicted, with a constant trend against particle mass flow rate. This is because the DPM model is not a 2-ways coupling algorithm, hence the particulate mass flow rate is assumed not to interact with the gas phase, i.e. the constant distribution. This assumption is valid for low particle volume fractions (<10%); in the current case levels between 5% and 40% were calculated. A fully Eulerian 2-way coupling CFD model for particle velocities levels similar to CoBlast does not exist in commercial packages; the importance of the experimental results by the PIV apparatus is therefore clear. They have revealed an initial particle stream distribution in the CoBlast process not possible to predict numerically. This information will represent a critical step forward towards the design of new and application-tailored nozzles in CoBlast.

6. Conclusion

The average velocity of aluminium oxide particles propelled by a CoBlast nozzle at 3, 4 and 5 bar was measured. The increase in velocity with pressure was quantified and a number of regions of interest for scientific investigation were highlighted. It was clear from the experimental measurements that the particulate velocity distribution at the nozzle exit is linked to the particle mass flow rate injected at the inlet. Thus, increasing the particle feed rate, for example with the aim of accelerating the coating formation, will result in a less efficient abrasive action. Results were compared against CFD models, which over-predicted the experimental measurements. The critical assumptions in ANSYS Fluent v14.5-DPM to cause this were discussed. These included one-way coupling, not suitable for the modelling of solid phase volume fractions >10%, therefore under CoBlast working parameters. Using an advanced PIV set-up, it was therefore possible to generate data at a level of accuracy currently not achievable numerically with simulations, and that can be used for the design, optimization and characterization of new generation CoBlast nozzles.

Acknowledgements

The authors would like to express their gratitude to the technical staff in TCD, and to Dr. Tim Persoons for the valuable support towards the achievements in this research.

References

[1] L. Baptiste, N. van Landschoot, G. Gleijm, J. Priede, J. Schade van Westrum, H. Velthuis, and T.-Y. Kim, "Electromagnetic levitation: A new technology for high rate physical vapour deposition of coatings onto metallic strip," *Surf. Coatings Technol.*, vol. 202, no. 4–7, pp. 1189–1193, Dec. 2007.

[2] K. S. Fancey, "A coating thickness uniformity model for physical vapour deposition systems: overview," *Surf. Coatings Technol.*, vol. 71, no. 1, pp. 16–29, Feb. 1995.

[3] D. M. Mattox, *Handbook of physical vapor deposition (PVD) processing*. William Andrew, 2010.

[4] P. Morrell and D. S. Rickerby, "Advantages / Disadvantages of Various TBC Systems as perceived by the Engine Manufacturer," Derby, 1998.

[5] N. J. Archer, "Chemical Vapour Deposition," *Phys. Technol.*, vol. 10, no. 4, 1979.

[6] A. M. Oladoye, J. G. Carton, and A. G. Olabi, "Evaluation of CoBlast Coated Titanium Alloy as Proton Exchange Membrane Fuel Cell Bipolar Plates," *J. Mater.*, vol. 2014, pp. 1–10, 2014.

[7] C. F. Dunne, B. Twomey, L. O'Neill, and K. T. Stanton, "Co-blasting of titanium surfaces with an abrasive and hydroxyapatite to produce bioactive coatings: substrate and coating characterisation.," *J. Biomater. Appl.*, vol. 28, no. 0, pp. 767–78, 2014.

[8] J. N. Barry, B. Twomey, A. Cowley, L. O'Neill, P. J. McNally, and D. P. Dowling, "Evaluation and comparison of hydroxyapatite coatings deposited using both thermal and non-thermal techniques.," *Surf. Coatings Technol.*, vol. 226, pp. 82–91, Jul. 2013.

[9] G. D. Byrne, L. O'Neill, B. Twomey, and D. P. Dowling, "Comparison between shot peening and abrasive blasting processes as deposition methods for hydroxyapatite coatings onto a titanium alloy.," *Surf. Coatings Technol.*, vol. 216, pp. 224–231, Feb. 2013.

[10] D. Fleming, L. O'Neill, G. Byrne, N. Barry, and D. P. Dowling, "Wear resistance enhancement of the titanium alloy Ti–6Al–4V via a novel co-incident microblasting process.," *Surf. Coatings Technol.*, vol. 205, no. 21–22, pp. 4941–4947, Aug. 2011.

[11] L. O'Neill, C. O'Sullivan, P. O'Hare, L. Sexton, F. Keady, and J. O'Donoghue, "Deposition of substituted apatites onto titanium surfaces using a novel blasting process.," *Surf. Coatings Technol.*, vol. 204, no. 4, pp. 484–488, Nov. 2009.

[12] J. N. Barry, A. Cowley, P. J. McNally, and D. P. Dowling, "Influence of substrate metal alloy type on the properties of hydroxyapatite coatings deposited using a novel ambient temperature deposition technique.," *J. Biomed. Mater. Res.*, vol. 102, no. 3, pp. 871–9, Mar. 2014.

[13] A. Wennerberg, A. Ektessabi, T. Albrektsson, C. Johansson, and B. Andersson, "A 1 year follow-up of implants of differing surface roughness placed in rabbit bone," *Int. J. Oral Maxillofac. Implant.*, vol. 12, no. 4, pp. 486–494, 1997.

[14] H. Nakada, T. Sakae, R. Z. LeGeros, J. P. LeGeros, T. Suwa, and K. Numata, YasukoKobayashi, "Early Tissue Response to Modified Implant Surfaces Using Back Scattered Imaging," *Implant Dent.*, vol. 16, no. 3, pp. 281–289, 2007.

[16] C. F. Dunne, B. Twomey, C. Kelly, J. C. Simpson, and K. T. Stanton, "Hydroxyapatite and fluorapatite coatings on dental

screws: effects of blast coating process and biological response," *J. Mater. Sci. Mater. Med.*, vol. 26, 2015.

[17] M. Raffel, C. E. Willert, S. T. Wereley, and J. Kompenhans, *Particle Image Velocimetry: A Practical Guide.*, Second. Springer, 1998.

[18] R. J. Adrian, "Twenty years of particle image velocimetry," *Exp. Fluids*, vol. 39, no. 2, pp. 159–169, Jul. 2005.

[19] J. Westerweel, "Fundamentals of digital particle image velocimetry," *Meas. Sci. Technol.*, vol. 8, pp. 1379–1392, 1997.

[20] R. J. Adrian, "Dynamic ranges of velocity and spatial resolution of particle image velocimetry," *Meas. Sci. Technol.*, vol. 8, pp. 1393–1398, 1999.

[21] A. K. Prasad, "Particle image velocimetry," *Curr. Sci.*, vol. 79, no. 1, pp. 51–60, 2000.

[22] H. K. Versteeg and W. Malalasekera, *An Introduction to Computational Fluid Dynamics*, Second., vol. M. Pearson, 1995.

[23] A. Inc, "ANSYS v14.5 Help - // User's Guide," in *Fluent Users Guide*, .

[24] M. Stanislas and J. C. Monnier, "Practical aspects of image recording in particle image velocimetry," *Meas. Sci. Technol.*, vol. 8, pp. 1417–1426, 1999.

[25] G. S. Settles and S. Garg, "A scientific view of the productivity of abrasive blasting nozzles," *J. Therm. Spray Technol.*, vol. 5, pp. 35–41, 1996.